



Journal of Applied Sciences

ISSN 1812-5654

science
alert

ANSI*net*
an open access publisher
<http://ansinet.com>

Determination of Gravity Anomalies over the Arabian Sea

¹Ahmed Abdo Ali, ²Liu Jing Nan and ³Jiang Wei Peng

¹School of Geodesy and Geomatics, Wuhan University, 129 Luoyu road, Wuhan 430079, China

²Academician, President of Wuhan University, Wuhan, China

³School of Geodesy and Geomatics, Wuhan University, Wuhan, China

Abstract: Gravity anomalies derived from satellite altimetry are progressively taking the place of ship-borne gravity for many marine geo-scientific investigations this paper compares the marine gravity anomalies-derived from multi-mission satellite altimetry-with gravity anomalies implied by the EGM96 global geopotential model. The results show some significant differences among these gravity data sources. Ocean satellite altimetry implied free-air gravity anomalies have had the shortest wavelength removed during the processing to generate the optimal solution between multiple radar altimeter missions. Compute gravity anomalies by LSC using along-track, differenced geoidal heights and height slopes. Gravity Anomalies over the Arabian Sea (latitudes: 0-25°N and longitudes: 35-70°E) is computed by using along track deflections of vertical and grid along track deflections of vertical using Shepard's method of gridding procedure and finally the gravity anomalies were computed using the inverse Vening-Meinesz formula we used altimeter data from Topex/Poseidon, Jason1, Geosat, ERS1 and ERS2 missions.

Key words: Satellite altimetry, mean sea surface, deflection of the vertical, gravity anomalies

INTRODUCTION

The main goal of satellite altimetry is the study and observation of the processes and properties of the marine environment, so that when utilizing altimetry data the monitoring of phenomena like the mean sea level variations and changes, the ice transfer, the wind speed, the wave height and the water temperature would be feasible. It is possible, through various techniques, to derive information about the marine gravity field and the ocean tides as well (Emadi *et al.*, 2003).

Altimetric measurements have a vital importance for geodesy, since we are able to provide a direct measurement of the main estimation quantity of geodesy i.e., geoid heights. Since the altimetric observations, the Sea Surface Heights (SSHs), correspond to the separation of the sea surface from the reference ellipsoid is very close to geoid undulations. The difference between Mean sea surface height and geoid is called Sea Surface Topography (SST). The deflections of the vertical are calculated directly by differentiating the sea surface height observations in the along track direction, or by differentiating the geoid undulations in the regular grid and then the free-air gravity anomalies, the difference between the magnitude of the actual gravity (W_0) on the

geoid and the magnitude of the normal gravity (γ_0) on the ellipsoid' were computed using the inverse Vening-Meinesz formula.

2-D of deflections of vertical components and gravity anomaly with satellite altimetry data: Deflection of vertical is defined as the spatial angle between the normal gravity vector on the reference ellipsoid and the actual gravity vector on the geoid (θ).

It can also be interpreted as the maximum slope of the geoid with respect to the reference ellipsoid at the point of interest.

$$\xi = \frac{1}{r} \frac{\partial N}{\partial \phi} \quad (1)$$
$$\eta = -\frac{1}{r \cos \phi} \frac{\partial N}{\partial \lambda}$$

By using gradients of the sea surface height many of the long wavelength altimetry error sources are limited. An obvious advantage is that the task of having to perform a crossover reduction can be avoided. The deflections of the vertical are calculated directly by differentiating the sea surface height observations in the along track direction and then computing the deflections

of the vertical (ξ, η) from equation (1) At the crossover location where ascending and descending ground tracks intersect from either the same or different satellites a much more stable determination of the slopes can be obtained.

Vertical deflections from along-track slopes: Taking the first horizontal derivatives of the altimeter-sensed sea surface heights along-track yields the negative deflections of the vertical at the geoid. These are interpolated onto a regular grid and can be converted to gravity anomalies using the inverse Vening-Meinesz formula.

The derivative of the geoid height N with respect to time t along the ascending profile is (Smith and Sandwell, 1994):

$$\dot{N}_a = \frac{\partial N_a}{\partial t} = \frac{\partial N_a}{\partial \phi} \dot{\phi}_a + \frac{\partial N_a}{\partial \lambda} \dot{\lambda}_a \quad (2)$$

and along the descending profile is:

$$\dot{N}_d = \frac{\partial N_d}{\partial t} = \frac{\partial N_d}{\partial \phi} \dot{\phi}_d + \frac{\partial N_d}{\partial \lambda} \dot{\lambda}_d \quad (3)$$

Where

ϕ, λ are the geodetic latitude and geodetic longitude of data points, respectively. At the crossover point the following relationships are accurate to better than 0.1%.

$$\begin{aligned} \dot{\phi}_a &= -\dot{\phi}_d \\ \dot{\lambda}_a &= \dot{\lambda}_d \end{aligned} \quad (4)$$

The geoid gradient (deflection of the vertical) is obtained by solving (1) using (4). Then we can write:

$$\frac{\partial N}{\partial \phi} = \frac{1}{2\phi} (\dot{N}_a + \dot{N}_d) \quad (5)$$

$$\frac{\partial N}{\partial \lambda} = \frac{1}{2|\dot{\lambda}|} (\dot{N}_a - \dot{N}_d) \quad (6)$$

When two or more satellites with different orbital inclinations are available, the situation is slightly more complex but more stable.

Gridding the deflection of vertical components: The computed deflections of vertical components were discrete values, which were randomly distributed over Arabian sea and that the distances between them were

not uniform. As required by FFT techniques that the input data should be uniformly spaced on a regular grid (Dadzie, 2005).

We used Shepard's method of gridding procedure to interpolate values of deflection of vertical components at locations where no data existed, using a grid spacing of 2.5' arc-minute in both longitude and latitude directions. the computational steps as follow:

Knowing the coordinates of the discrete crossover point positions (ϕ_i, λ_i) in a spherical coordinate system (ϕ, λ) and the corresponding values of the components of the deflection of vertical, $f_i = f(\phi_i, \lambda_i)$ ($i = 1, 2, \dots, N$) the differences in longitude ($\Delta\lambda_i$) and latitude ($\Delta\phi_i$) between the coordinates of each of the discrete crossover points (ϕ_i, λ_i) within a grid cell and the coordinates (ϕ_0, λ_0) of the grid node (i.e., the centre point of the grid cell where Z value is to be interpolated) are computed;

$$\begin{cases} \Delta\phi_i = \phi_i - \phi_0 \\ \Delta\lambda_i = \lambda_i - \lambda_0 \end{cases} \quad (7)$$

Where r_i is the distance, between the grid node, termed the computation point P and the i th discrete crossover point within the cell, termed the running point Q , is computed by :

$$r_i = 2R \sin\left(\frac{\Psi_i}{2}\right) \quad (8)$$

where R is the mean radius of the Earth, Ψ , is the spherical distance between P and Q and

$$\sin^2 \frac{\Psi}{2} = \sin^2 \frac{\Delta\phi}{2} + \sin^2 \frac{1}{2} \Delta\lambda \cos \phi_P \cos \phi_Q \quad (9)$$

the weight function can be calculated as (Jiang, 2001) :

$$\phi(\phi, \lambda) = \begin{cases} \frac{1}{r} & 0 < r \leq \frac{S}{3} \\ \frac{27}{4S} \left(\frac{r}{S} - 1\right)^2 & \frac{S}{3} < r \leq S \\ 0 & r > S \end{cases} \quad (10)$$

where r is the search radius and S is the spherical cap, which was set at 2°. The interpolator was finally given by:

$$z = F(\phi, \lambda) = \begin{cases} \frac{\sum_{i=1}^N f^{\mu}[\phi(r_i)]}{\phi^{\mu}(r_i)} & r_i \neq 0 \\ f_i & r_i = 0 \end{cases} \quad (11)$$

where N is the number of data points used in fitting the interpolated value at the grid node and μ is the smoothing factor, which was set at 2 for this study.

Computation gravity anomaly using inverse vening-meinesz formula: The concepts of determining marine gravity anomalies from satellite radar altimetry are as follows. The altimeter essentially measures the distance between the satellite and the instantaneous sea surface along the nadir using pulse-limited radar at a series of footprints along the sub-satellite tracks (Fu and Cazenave, 2001).

The Inverse Vening Meinesz formula used in this study to compute gravity anomalies using altimeter-derived components of deflection of vertical (Eqs. 1-5) as input data and is given as (Cheng *et al.*, 2001; Hwang, 1998):

$$\Delta g = \frac{\gamma}{4\pi R} \iint_{\sigma} \left(3 \csc \psi - \csc \psi \csc \frac{\Psi}{2} - \tan \frac{\Psi}{2} \right) \frac{\partial N}{\partial \psi} d\sigma \quad (12)$$

where the component of deflection of vertical along the azimuth α is related to the geoid slope ($\frac{\partial N}{\partial \psi}$)

$$\frac{\partial N}{\partial \psi} = R(\xi \cos \alpha + \eta \sin \alpha) \quad (13)$$

where R is the mean radius of the earth ξ and are η the altimeter-derived north-south and east-west components of the deflection of the vertical, respectively.

$$\sin \alpha = -\frac{\cos \varphi \sin(\lambda_p - \lambda)}{\sin \psi} \quad (14)$$

$$\alpha = \frac{\cos \varphi_p \sin \varphi - \sin \varphi_p \cos \varphi \cos(\lambda_p - \lambda)}{\sin \psi} \quad (15)$$

substituting Eq. (13) into Eq. (12) yields

$$\Delta g(\varphi_p, \lambda_p) = \frac{\gamma}{4\pi} \iint_{\sigma} \left(3 \csc \psi - \csc \psi \csc \frac{\Psi}{2} - \tan \frac{\Psi}{2} \right) (\xi \cos \alpha + \eta \sin \alpha) d\sigma \quad (16)$$

$$\Delta g(\varphi_p, \lambda_p) = \frac{\gamma}{4\pi} \iint_{\sigma} \left[\xi \cos \alpha \left(3 \csc \psi - \csc \psi \csc \frac{\Psi}{2} - \tan \frac{\Psi}{2} \right) + \eta \sin \alpha \left(3 \csc \psi - \csc \psi \csc \frac{\Psi}{2} - \tan \frac{\Psi}{2} \right) \right] d\sigma \quad (17)$$

considering the Eq. (14) and (15) Eq. (17) is written as:

$$\Delta g(\varphi_p, \lambda_p) = \frac{\gamma}{4\pi} \iint_{\sigma} (\xi IV_{\xi} + \eta IV_{\eta}) d\sigma \quad (18)$$

where

$$IV_{\xi} = \cos \alpha \left(3 \csc \psi - \csc \psi \csc \frac{\Psi}{2} - \tan \frac{\Psi}{2} \right) = \left(\frac{\cos \varphi_p \sin \varphi - \sin \varphi_p \cos \varphi \cos(\lambda_p - \lambda)}{\sin \psi} \right) \left(3 \csc \psi - \csc \psi \csc \frac{\Psi}{2} - \tan \frac{\Psi}{2} \right) \quad (19)$$

$$= -\left(\frac{\cos \varphi \sin(\lambda_p - \lambda)}{\sin \psi} \right) \left(3 \csc \psi - \csc \psi \csc \frac{\Psi}{2} - \tan \frac{\Psi}{2} \right) \quad (20)$$

and

$$\sin(\psi/2) = \left[\sin^2 \frac{1}{2}(\varphi_p - \varphi) + \sin^2 \frac{1}{2}(\lambda_p - \lambda) \cos \varphi_p \cos \varphi \right]^{1/2} \quad (21)$$

so

the 1D convolution of Eq. (17) is expressed as:

$$\begin{aligned} \Delta g(\varphi, \lambda) &= \frac{\gamma}{4\pi} \iint_{\sigma} [\xi(\varphi, \lambda) IV_{\xi}(\varphi, \varphi, \lambda_p - \lambda) + \eta(\varphi, \lambda) IV_{\eta}(\varphi, \varphi, \lambda_p - \lambda)] d\sigma \\ &= \frac{\gamma}{4\pi} \int_{\varphi} \{ [\xi(\varphi, \lambda) \cos \varphi] * IV_{\xi}(\varphi, \varphi, \lambda_p - \lambda) + [\eta(\varphi, \lambda) \cos \varphi] * IV_{\eta}(\varphi, \varphi, \lambda_p - \lambda) \} d\varphi \\ &= \frac{\gamma}{4\pi} F_1^{-1} \{ \int_{\varphi} \{ [\xi(\varphi, \lambda) \cos \varphi] F_1 [IV_{\xi}(\varphi, \varphi, \lambda_p - \lambda)] + [\eta(\varphi, \lambda) \cos \varphi] F_1 [IV_{\eta}(\varphi, \varphi, \lambda_p - \lambda)] \} d\varphi \} \end{aligned} \tag{22}$$

$$cs = \cos \varphi_p \sin \varphi = \frac{1}{2} [\sin(\varphi_p + \varphi) - \sin(\varphi_p - \varphi)] = \frac{1}{2} [\sin(2\varphi_M) - \sin(\varphi_p - \varphi)] \tag{23}$$

$$cs = \sin \varphi_p \cos \varphi = \frac{1}{2} [\sin(\varphi_p + \varphi) + \sin(\varphi_p - \varphi)] = \frac{1}{2} [\sin(2\varphi_M) + \sin(\varphi_p - \varphi)] \tag{24}$$

The corresponding spectral expressions for 2D spherical convolution and 2D-FFT of Eq. (17) given below:

$$\Delta g(\varphi_p, \lambda_p) = \frac{\gamma}{4\pi} \iint_{\sigma} (\xi IV_{\xi} + \eta IV_{\eta}) d\sigma \tag{25}$$

where

$$\begin{aligned} IV_{\xi} &= \cos \alpha (3 \csc \psi - \csc \psi \csc \frac{\Psi}{2} - \text{tg} \frac{\Psi}{2}) \\ &= \left[\frac{\cos \varphi_p \sin \varphi - \sin \varphi_p \cos \varphi \cos(\lambda_p - \lambda)}{\sin \psi} \right] \cdot (3 \csc \psi - \csc \psi \csc \frac{\Psi}{2} - \text{tg} \frac{\Psi}{2}) \end{aligned} \tag{26}$$

$$IV_{\eta} = \sin \alpha (3 \csc \psi - \csc \psi \csc \frac{\Psi}{2} - \text{tg} \frac{\Psi}{2}) = - \frac{\cos \alpha \sin(\lambda_p - \lambda)}{\sin \psi} \cdot (3 \csc \psi - \csc \psi \csc \frac{\Psi}{2} - \text{tg} \frac{\Psi}{2}) \tag{27}$$

$$\begin{aligned} \Delta g(\varphi, \lambda) &= \frac{\gamma}{4\pi} \iint_{\sigma} [\xi(\varphi, \lambda) IV_{\xi}(\varphi_p - \varphi, \lambda_p - \lambda) + \eta(\varphi, \lambda) IV_{\eta}(\varphi_p - \varphi, \lambda_p - \lambda)] d\sigma \\ &= \frac{\gamma}{4\pi} \{ [\xi(\varphi, \lambda) \cos \varphi] * IV_{\xi}(\varphi_p - \varphi, \lambda_p - \lambda) + [\eta(\varphi, \lambda) \cos^2 \varphi] * IV_{\eta}(\varphi_p - \varphi, \lambda_p - \lambda) \} \\ &= \frac{\gamma}{4\pi} F_2^{-1} \{ F_2 [\xi(\varphi, \lambda) \cos \varphi] F_2 [IV_{\xi}(\varphi, \lambda)] + F_2 [\eta(\varphi, \lambda) \cos^2 \varphi] F_2 [IV_{\eta}(\varphi, \lambda)] \} \end{aligned} \tag{28}$$

where and represent the 2D-FFT operator and its inverse. With Eq. (28) the gravity anomalies at all gridded points are computed simultaneously.

RESULTS AND ANALYSES

The differences between the altimeter-derived gravity anomalies (Fig. 1 and 2) and the EGM96-derived gravity anomalies are equal to the residual gravity anomalies computed utilizing the inverse Vening Meinsz formula and they represent the short-wavelength component of the gravity anomaly signal. Table 1 and 2 show the descriptive statistics of the differences between the altimeter-derived

Table 1: Statistics of the differences between EGM96-generated and altimeter-derived gravity anomalies via 1D-FFT over the Arabian Sea (unit, mgal)

Mission	Max	Min	Mean	RMS	STD
TP	141.618	-103.162	0.426015	15.1500	15.1440
ERS1	121.759	-156.492	-0.005573	12.4816	12.4816
ERS2	166.942	-178.027	0.44407	16.3950	16.3859
GEOSAT	142.005	-168.891	0.414398	17.8753	17.8705
JASON1	136.480	-144.267	0.401627	14.0308	14.0250

Table 2: Statistics of the differences between EGM96-generated and altimeter-derived gravity anomalies via 2D-FFT over the Arabian Sea (unit, mgal)

Mission	Max	Min	Mean	RMS	STD
TP	144.351	-98.0808	0.429878	14.8132	14.8070
ERS1	110.042	-144.869	0.00016867	12.0917	12.0917
ERS2	168.333	-180.490	0.536660	16.1214	16.1125
GEOSAT	145.467	-170.973	0.417135	17.5834	17.5784
JASON1	131.253	-136.704	0.404035	13.7116	13.7057

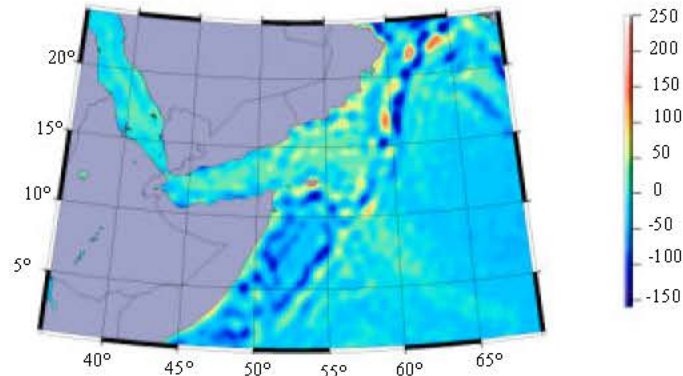


Fig. 1: 2.5'x2.5' Map of altimeter-derived gravity anomalies

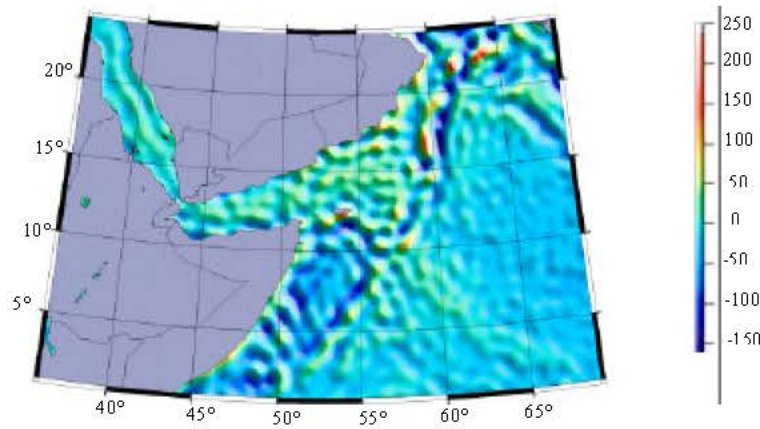


Fig. 2: 2.5'x2.5' 3D map of altimeter-derived gravity anomalies

Table 3: Statistics of the deflection of vertical over the Arabian Sea via 1D-FFT(unit, mgal)

Mission	Max	Min	Mean	RMS	STD
TP	223.486	-169.957	-4.10177	36.2877	36.0551
ERS1	255.088	-160.005	-4.53336	34.5176	34.2186
ERS2	208.173	-179.186	-4.12514	34.7438	34.4980
GEOSAT	233.879	-184848	-4.1133	38.2838	38.0622
JASON1	208.173	-179.186	-4.12514	34.7438	34.4980

Table 4: Statistics of the deflection of vertical over the Arabian Sea via 2D-FFT(unit, mgal)

Mission	Max	Min	Mean	RMS	STD
TP	218.473	-163.896	-4.0979	36.0052	35.7713
ERS1	239.126	-156.763	-4.52796	34.2265	33.9257
ERS2	201.777	-172.238	-4.12276	34.5154	34.2683
GEOSAT	231.617	-176.521	-4.11065	37.9690	37.7459
JASON1	201.777	-172.238	-4.12276	34.5154	34.2683

gravity anomalies and the EGM96- derived gravity anomalies for 1D and 2D-spherical FFT, respectively, Table 3 and 4 show the statistics of the gravity anomalies over the Arabian Sea computed from deflections of vertical via 1D and 2D-spherical FFT, respectively.

CONCLUSIONS

This study describes the procedure and accuracy for marine gravity anomalies over Arabian Sea from multi-satellite altimetry. for the present research, it could concluded that the influence of the Dynamic Ocean Topography on the deflection of vertical should be taken into account in order to improve the accuracy of the determination of gravity anomalies. The gridded residual vertical deflections over unobserved area can be supplied by the corresponding model value when the inverse Vening-Meinesz formula is used to derive the marine gravity anomalies.

REFERENCES

Cheng, L.J., N.J. Sheng, C.J. Yong and C.D. Bo., 2001. Determination of gravity anomalies over the South China sea by combination of Topex/Poseidon, ERS2 and Geosat Altimeter Data, *acta geodaetica and catographica sinica*, 30: 197-201.

- Dadzie, I., 2005. Derivation of gravity anomalies and geoid over the South China sea from multi-satellite altimetry data. Ph.D Thesis.
- Emadi, S.R., M. Najafi-Alamdari, K.N. Toosi and M. Sedighi, 2003. Determination of the earth gravity field parameters in persian gulf and Oman sea with the satellite altimetry data. Islamic Azad University, Tehran, South Unit.
- Fu, L.L. and A. Cazenave, 2001. Satellite Altimetry and Earth Sciences: A Handbook of Techniques and Applications, International Geophysics Sciences. Vol. 69, Academic Press, San Diego, USA., pp: 463.
- Hwang, C., 1998. Inverse vening meinesz formula and deflection-geoid formula: Applications to the predictions of gravity and geoid over the South China Sea. *J. Geodesy*, 72: 304-312.
- Jiang, W.P., 2001. The application of satellite altimetry in geodesy. Ph.D Thesis.
- Smith, W.H.F. and D.T Sandwell, 1994. Bathymetric prediction from dense satellite altimetry and sparse shipboard bathymetr. *J. Geophys. Res.*, 99: 21803-21824.